

Exploring the Dynamics of CME-Driven Shocks by Comparing Numerical Modeling and Observations

Meng Jin¹, Gang Li², Nariaki Nitta¹, Wei Liu^{1,3}, Vahé Petrosian⁴, Ward Manchester⁵, Christina Cohen⁶, Frederic Effenberger^{3,7}, Zheyi Ding⁸, Melissa Pesce-Rollins⁹, Nicola Omodei⁴ and Nat Gopalswamy¹⁰

¹ Lockheed Martin Solar and Astrophysics Lab (LMSAL), Palo Alto, CA, USA

² General Linear Space Plasma Lab LLC, Foster City, CA, USA

³ Bay Area Environmental Research Institute (BAERI), Mountain View, CA, USA

⁴ Stanford University, Stanford, CA, USA

⁵ University of Michigan Ann Arbor, Ann Arbor, MI, USA

⁶ California Institute of Technology, Pasadena, CA, USA

⁷ Ruhr University Bochum (RUB), Bochum, Germany

⁸ KU Leuven, Leuven, Belgium

⁹ Istituto Nazionale di Fisica Nucleare (INFN), Sezione di Pisa, Pisa, Italy

¹⁰ NASA Goddard Space Flight Center, Greenbelt, MD, USA

Abstract. Shocks driven by coronal mass ejections (CMEs) are primary drivers of gradual solar energetic particle (SEP) events, posing significant risks to space technology and astronauts. Concurrently, particles accelerated at these shocks may also propagate back to the Sun, potentially generating gamma-ray emissions through pion decay. We incorporated advanced modeling and multi-messenger observations to explore the role of CME-driven shocks in gamma-ray emissions and SEPs. Motivated by Fermi-LAT long-duration solar flares, we used the AWSoM MHD model to investigate the connection between the shocks and the properties of observed gamma-ray emissions. By coupling the AWSoM with iPATH model, we evaluate the impact of shock evolution complexity near the Sun on SEP intensity and spectra. Our result points to the importance of accurate background coronal and solar wind modeling, as well as detailed observations of CME source regions, in advancing our understanding of CME-driven shocks and the dynamics of associated energetic particles.

Keywords. Solar Gamma Ray Flares, Coronal Mass Ejections, Energetic Particles, Particle Transport

1. Introduction

Shocks driven by Coronal Mass Ejections (CMEs) play an important role in accelerating particles. Particles cross the shock front back and forth due to interaction with magnetic turbulence and gain energy through the diffusive shock acceleration mechanism (e.g. [Axford et al. 1977](#)). Accelerated particles that escape upstream can propagate along the interplanetary magnetic field lines and are detected in situ as Solar Energetic Particles (SEPs), posing significant risks to both technology and astronauts in space.

Conversely, particles accelerated at the shock front can also escape downstream, traveling back to the Sun where they may generate γ -ray emissions through pion decay with the ambient plasma in the photosphere. The sustained/long-duration γ -ray emission (SGRE) events observed by the Fermi Large Area Telescope (LAT: [Atwood et al. 2009](#)) provide evidence supporting this “shock scenario”, which potentially opens a new window for observing shock-accelerated particles in γ -rays. [Gopalswamy et al. \(2018\)](#) found a strong correlation between the SGRE events and Type II radio bursts, with a linear relationship between their durations, suggesting a common shock accelerating both protons and electrons that are respectively responsible for such emissions. In a recent study, [Gopalswamy et al. \(2021\)](#) found that the

number of 500 MeV protons from the SGRE events is correlated with the protons propagating into space as SEPs.

In both cases, the CME-driven shock and its dynamical evolution through the inhomogeneous solar wind are crucial for understanding the particle acceleration and transport processes involved. Employing data-driven global magnetohydrodynamics (MHD) models enables the quantitative reconstruction of the global corona and the dynamic evolution of CME-driven shocks, offering unique insights into the role of CMEs in these phenomena (e.g. Plotnikov et al. 2017; Jin et al. 2018). In addition, to properly model SEP events, the MHD models need to be coupled with particle acceleration and transport models (e.g. Li et al. 2021). This study aims to investigate both γ -ray and SEP events to delve into the dynamics of CME-driven shocks by comparing advanced modeling and observations results.

The paper is structured as follows: Section 2 provides an overview of the models used; Section 3 presents the main results; discussions are in Section 4, followed by the summary and conclusions in Section 5.

2. Model

To reconstruct the background solar corona and wind, we use the Alfvén Wave Solar Model (AWSoM; van der Holst et al. 2014), a data-driven global MHD model within the Space Weather Modeling Framework (Tóth et al. 2012). By incorporating a physically consistent treatment of wave reflection, dissipation, and heat partitioning between electrons and protons, AWSoM has been demonstrated to reproduce high-fidelity global solar corona conditions (e.g., Sokolov et al. 2013; Jin et al. 2017b; Sachdeva et al. 2019). Specifically, the inner boundary condition of the magnetic field is specified with full-surface magnetic maps. Alfvén waves are driven at the inner boundary with a Poynting flux that scales with the surface magnetic field. The solar wind is heated by Alfvén wave dissipation and accelerated by thermal and Alfvén wave pressure. While electrons and protons are collisionally coupled, their temperatures are computed separately. This treatment is critical for reproducing physically correct CME-driven shocks (Jin et al. 2013).

To generate a CME eruption, we use a simulation tool called the Eruptive Event Generator Gibson-Low (EEGGL, now available at NASA CCMC, Jin et al. 2017a; Borovikov et al. 2017) that inserts a Gibson-Low (GL) flux rope (Gibson and Low 1998) into the corona. It automatically determines the flux rope parameters with a handful of quantities given by observations (i.e., magnetogram and CME speeds) so that the modeled CMEs can travel at the desired speeds near the Sun.

To model SEP events, we further couple the AWSoM MHD model with the improved Particle Acceleration and Transport in the Heliosphere model (iPATH; Hu et al. 2017). iPATH numerically solves the particle acceleration at the shock and transport in the solar wind with both along- and cross-field diffusion. One unique feature of iPATH is the adoption of a 2D onion shell module which tracks the acceleration of particles and their subsequent convection and diffusion downstream of the shock. Li et al. (2021) extended the 2D shell structures to 3D using the AWSoM MHD shock and plasma inputs. In addition, an ensemble approach was developed to account for the model uncertainties in magnetic connectivity and shock profiles, i.e., multiple field lines were traced that were evenly distributed within 10° of a heliospheric observer.

3. Results

3.1. CME-driven Shock in Relation to Fermi SGRE Solar Flares

In this section, we show the modeling results for three Fermi SGRE events. Two of them (SOL2014-09-01 and SOL2021-07-17) are behind-the-limb (BTL) flares (Pesce-Rollins et al. 2015; Ackermann et al. 2017), in which the γ -ray emission region on the visible side of the

Sun was located *away* from the flare site behind the limb by tens of degrees in longitude. The other, equally intriguing, event is SOL2012-03-07, in which the Fermi γ -ray emission centroid *migrated with time* over the solar disk for 10 hours, long past the impulsive phase of the flare (Ajello et al. 2021).

In the SOL2014-09-01 event, the solar flare region was located 43° behind the east limb. However, Fermi-LAT detected γ -ray emissions on the front side of the Sun for ~ 2 hours. This event was associated with a fast CME with a speed $>1900 \text{ km s}^{-1}$. Figure 1 shows the MHD modeling result of this event. Specifically, Figure 1a depicts the magnetic field configuration after 16 minutes of the CME onset, while Figure 1b illustrates the simulated global EUV waves associated with the CME, where two different wave fronts are evident (marked in red arrows). The first wave front (to the right) is the fast-mode wave/shock driven by the eruption. The second one (to the left) is caused by the expanding CME flux rope shell (e.g., Jin et al. 2016). This double wave front feature is consistent with SDO/AIA observations of the event (e.g., Grechnev et al. 2018). Note that EUV waves are thought to be the low coronal counterparts of the CME-driven shock waves that propagate into the heliosphere. A recent study by Pesce-Rollins et al. (2022) demonstrated a strong correlation between the time derivative of the EUV wave intensity profile and Fermi/LAT γ -ray flux.

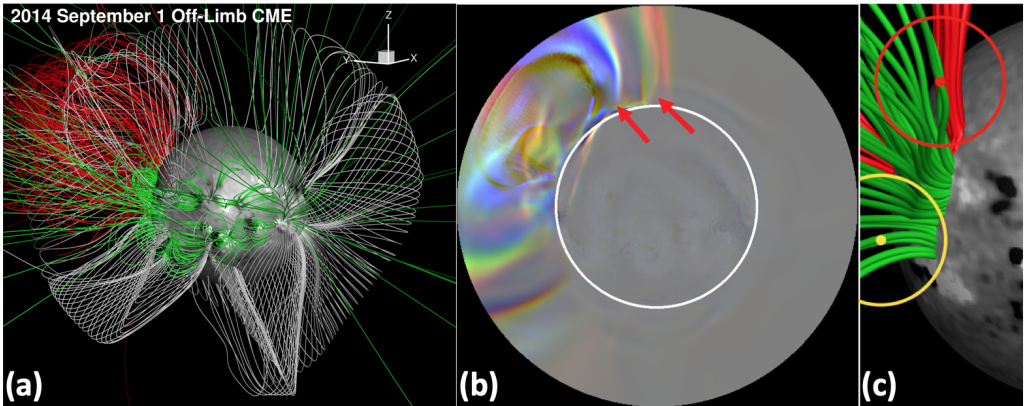


Figure 1. MHD modeling result of the SOL2014-09-01 Fermi BTL event. (a) Magnetic field configuration at $t = 16$ minutes after the flux rope eruption. The red and white field lines represent the flux rope and large-scale helmet streamers, respectively. The green field lines are selected surrounding active regions as well as open field lines. (b) Concurrent synthesized tri-color composite, running-ratio image for AIA 211 Å (red), 193 Å (green), and 171 Å (blue) channels showing the simulated EUV waves. (c) Selected field lines connecting to the CME shock (green) and source flare region (in red). The red and yellow dots with 95% uncertainty circles represent $>100 \text{ MeV}$ emission centroids identified previously by Ackermann et al. (2017) and updated recently in Ajello et al. (2021), respectively.

By modeling the evolution of the CME and the CME-driven shock over one hour, we derived the detailed history of 3D shock parameters including compression ratio, shock speed, shock Alfvén Mach number, and shock angle. We found that the shock compression ratio increases rapidly from ~ 1.8 at 10 minutes to ~ 4.6 at 20 minutes and then gradually decreases to ~ 3.7 at 60 minutes. This evolution trend is similar to the Fermi/LAT γ -ray intensity profile. Figure 1c shows the field lines connected to the CME shock (in green) and the source region (in red). Notably, in the recently updated Fermi solar flare catalog, the $>100 \text{ MeV}$ emission centroid has been revised further south (marked by a yellow circle), thus aligning more closely with the shock-connected field lines. See Jin et al. (2018) for detailed modeling results of this event.

SOL2021-07-17 is the most recent Fermi BTL event observed (Figure 2), and it exhibits the largest separation ($>50^\circ$) between the source region and the emission centroid of all the Fermi BTL events (Pesce-Rollins et al. 2022). Preliminary modeling results of the event are

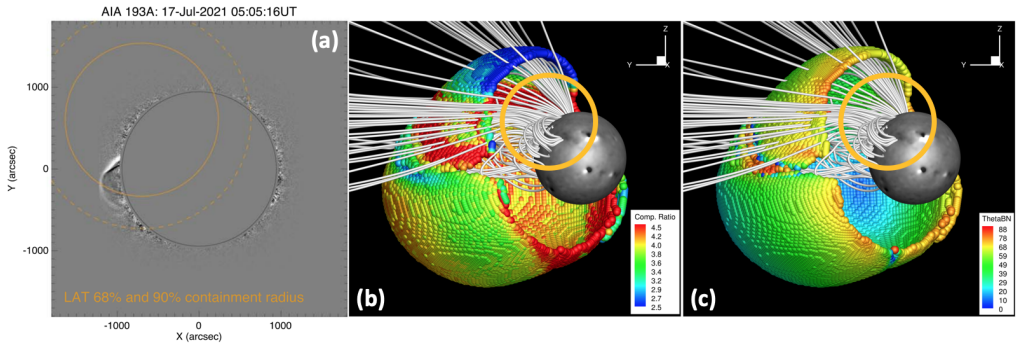


Figure 2. (a) Flare averaged Fermi-LAT emission centroid, shown as 90% (solid) and 68% (dashed) uncertainty circles, overlaid on the SDO/AIA 193 Å running difference image (adapted from [Pesce-Rollins et al. 2022](#)). (b)-(c) Modeled CME-driven shock compression ratio and θ_{Bn} at $t = 20$ minutes after eruption. The orange circle shows the same 90% uncertainty radius of the Fermi-LAT emission centroid as in (a).

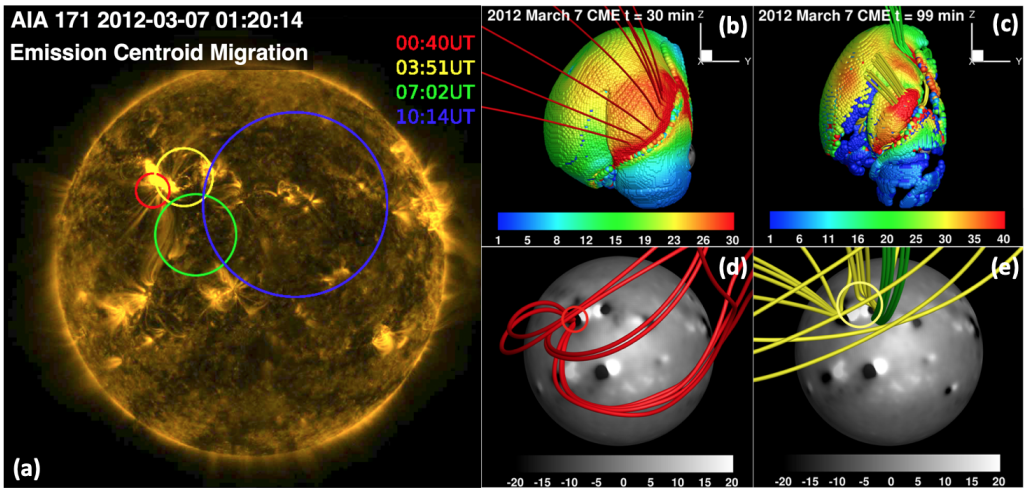


Figure 3. (a) Migration of the γ -ray emission centroid of the SOL2012-03-07 flare over 10 hours overlaid on an AIA 171 Å image at 00:40 UT. Circles show the 95% uncertainty. (b) & (c) Shock surface with the shock strength ($CR \cdot M_A$) in color derived from the simulation. (d) & (e) Magnetic field lines connecting to the strongest portion of the shock. The red and yellow circles are reproduced from (a), indicating good agreement of the LAT centroids with the roots of the field lines in corresponding colors.

shown in Figure 2b-c, which include the 3D shock compression ratio and shock angle from the simulation. The shock surface is notably non-spherical due to the inhomogeneous background solar wind, leading to significant variations in the shock parameters across different parts of the shock surface. Similar to the SOL2014-09-01 event, this event features shock-connecting open field lines that trace back to the Fermi emission centroid area. Additionally, the area where the shock intersects these field lines exhibits a quasi-perpendicular nature.

Lastly, we discuss the SOL2012-03-07 event. In this event Fermi observed the γ -ray emission centroid migration over the solar disk in 10 hours after flare impulsive phase (Figure 3a). This event is more challenging to model since there are two CMEs involved, separated by 1 hour. Although the two CMEs are from the same active region, they erupted from different parts of the polarity inversion line (PIL), with the first one started from the north, and the second one from the south (e.g., [Patsourakos et al. 2016](#)).

We model the SOL2012-03-07 event by initiating two separate GL flux ropes at different parts of PIL to match the AIA observation. To estimate strong shock location in the simulation,

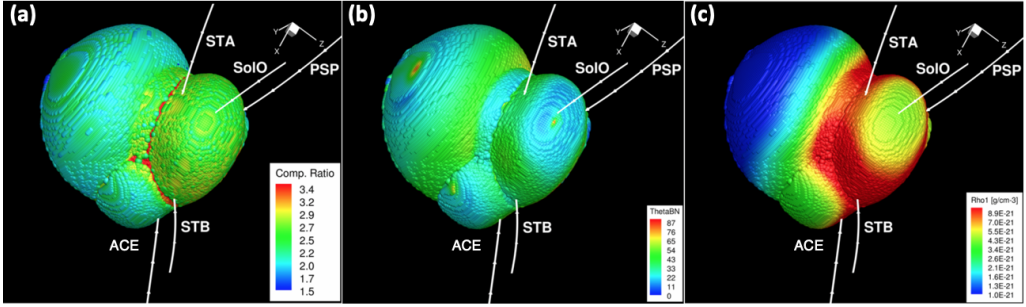


Figure 4. (a) The shock compression ratio, (b) shock angle, and (c) upstream plasma density along the shock surface at $t = 1$ hour in the 2021 October 28 SEP event. The white lines represent the field connectivity to different heliospheric observers.

we define a new parameter that combines compression ratio and Alfvén Mach number as shock strength measure. This approach enabled us to identify areas of strong shock on the shock surface and trace the field lines from those regions back to the Sun’s surface (Figure 3). At 30 minutes, these footpoints are situated south of the active region, aligning with the initial Fermi centroid marked in red. By 99 minutes into the simulation, the footpoints connected to the strong shock location begin moving northward, as indicated by the yellow circle, a movement consistent with observations.

Furthermore, we observed another strong shock region that developed at 99 minutes, with its footpoints situated near the Fermi centroid at 07:02, marked by a green circle. While we continue to work on the simulation beyond 100 minutes, these preliminary results indicate that the temporal evolution of footpoints, those which are connected to the strongest shock locations, aligns with the migration of the Fermi centroid during the first 100 minutes.

3.2. The Impact of CME-driven Shock Evolution on the in-situ SEP Intensity and Spectra

In this section, we discuss the impact of the CME-driven shock on the properties of SEPs measured in situ. As demonstrated in the previous section, the parameters of the CME-driven shock can vary significantly across different parts of the shock surface. Given that heliospheric observers at various locations are connected to different parts of the shock, the characteristics of the SEPs observed can be influenced by the properties of the specific shock segment to which they are connected. Understanding this relationship is crucial for better interpreting SEP observations.

One example is the 2021 October 28 SEP event, which was observed by Parker Solar Probe (PSP), STEREO-A, and SOHO/ACE with almost identical Fe/O ratio, even there is $\sim 60^\circ$ separation in longitude (Cohen et al. 2022). To better understand this distinctive characteristic, we modeled the associated CME-driven shock of this SEP event and calculated the field line connectivity to different observer locations including the SOHO/ACE, STA/B, SoIo, and PSP (Figure 4). Our preliminary results indicate that although the three observers (i.e., PSP, STEREO-A, and ACE) are connected to different parts of the shock, these areas nevertheless exhibit very similar properties, e.g., compression ratio, shock angle (see Figure 4a & b), as well as the upstream condition (see Figure 4c for upstream plasma density). This consistency might explain the similar Fe/O ratios observed at these locations.

Fe-rich events in gradual SEP events are thought to originate either directly from flare contributions (e.g., Cane et al. 2003, 2006) or from suprathermal flare particles that are preferentially accelerated by quasi-perpendicular shocks (Tylka et al. 2005). To evaluate the “quasi-perpendicular shock scenario”, eight SEP events were modeled using AWSoM MHD CME simulations, which allow for direct assessment of shock geometry — a feature difficult

to discern from near-Sun observations (Nitta et al. 2022). However, the preliminary results do not indicate a strong correlation between Fe-rich SEP events and quasi-perpendicular shocks. Suprathermal particles, which can be affected significantly by the inhomogeneity of the solar wind (Wijsen et al. 2023), or due to preceding impulsive SEP events, may play a significant role and warrant further investigation.

To quantitatively investigate the SEP events and their relationship to the CME-driven shocks, one needs both the global MHD model for tracking the CME-driven shock evolution through the background solar wind and the particle acceleration and transport model for calculating the transport of particles along the magnetic field lines. Most SEP models rely on simplified background solar wind and start at a larger distance from the Sun (e.g., 10 Rs). However, CME-driven shock could form at a height of just a few solar radii, with information on timing and formation height revealed through radio observations (e.g., Kozarev et al. 2011; Gopalswamy et al. 2013). There are previous attempts to include early phase shock evolution (e.g., Kozarev et al. 2013; Borovikov et al. 2018; Linker et al. 2019). By coupling two state-of-the-art models AWSoM and iPATH, Li et al. (2021) modeled the 2012 May 17 SEP event, including the very early phase. The new model successfully reproduced the SEP intensity profiles at both the Earth and STEREO-A locations as shown in Figure 5a-b. The new model also reproduces the high-energy end of SEP spectra up to 1 GeV observed by PAMELA (Bruno et al. 2018). The roll-over feature at high energy can be seen in both the observation and the simulation (Figure 5c). This study emphasizes the importance of early phase shock evolution on the particle acceleration and transport, especially on the high-energy end of SEP spectra. A new SEP forecasting model (SEPCaster) is under development based on this new capability (Whitman et al. 2023).

4. Discussion

Regarding the Fermi-LAT SGRE solar flares, our MHD simulations have shown some promising results supporting the “shock scenario”. However, recent observational studies challenge the notion that the shock is the origin of the γ -ray producing particles (e.g., de Nolfo et al. 2019; Bruno et al. 2023). de Nolfo et al. (2019) analyzed the particles interacting with the Sun as observed by Fermi/LAT and the SEPs observed at 1 AU from PAMELA in 14 SGRE solar flare events. Their findings suggest that the two particle populations are not correlated. Gopalswamy et al. (2021) offered a possible explanation by addressing two observational effects: the γ -ray flux might be underestimated in limb events, and the latitudinal widths of SEP distributions are energy-dependent.

There are alternative scenarios coexisting with the “shock scenario”. For example, flare-accelerated particles that are trapped locally within extended coronal loops after an eruption could be the source of the γ -ray producing particles (e.g., Ryan and Lee 1991; Hudson 2018). In the simulation of the SOL2014-09-01 event, we found some large-scale closed loops connected to the source region due to the interaction between the flux rope magnetic field and the global solar corona. These field lines could be significant for examining these trapped particles. In summary, further information remains to be explored in the simulations, and more advanced modeling is necessary to further differentiate between the scenarios mentioned above.

Another challenge to the “shock scenario” is the effect of magnetic mirroring. The strong magnetic mirroring, resulting from a high degree of convergence of magnetic field lines towards the Sun and extremely small loss cones, could potentially prevent particles from reaching the photosphere to produce γ -rays. To assess the impact of magnetic mirroring that inhibits particle transport back to the Sun, we calculated the evolution of the mirror ratio in the SOL2014-09-01 simulation. Using an approximate relationship between the escape time and mirror ratio (Mal'ushkin and Kulsrud 2001; Effenberger and Petrosian 2018), we determined that the particle escape timescale is shorter than the γ -ray emission period, which means a significant portion of the downstream protons can reach the photosphere and produce

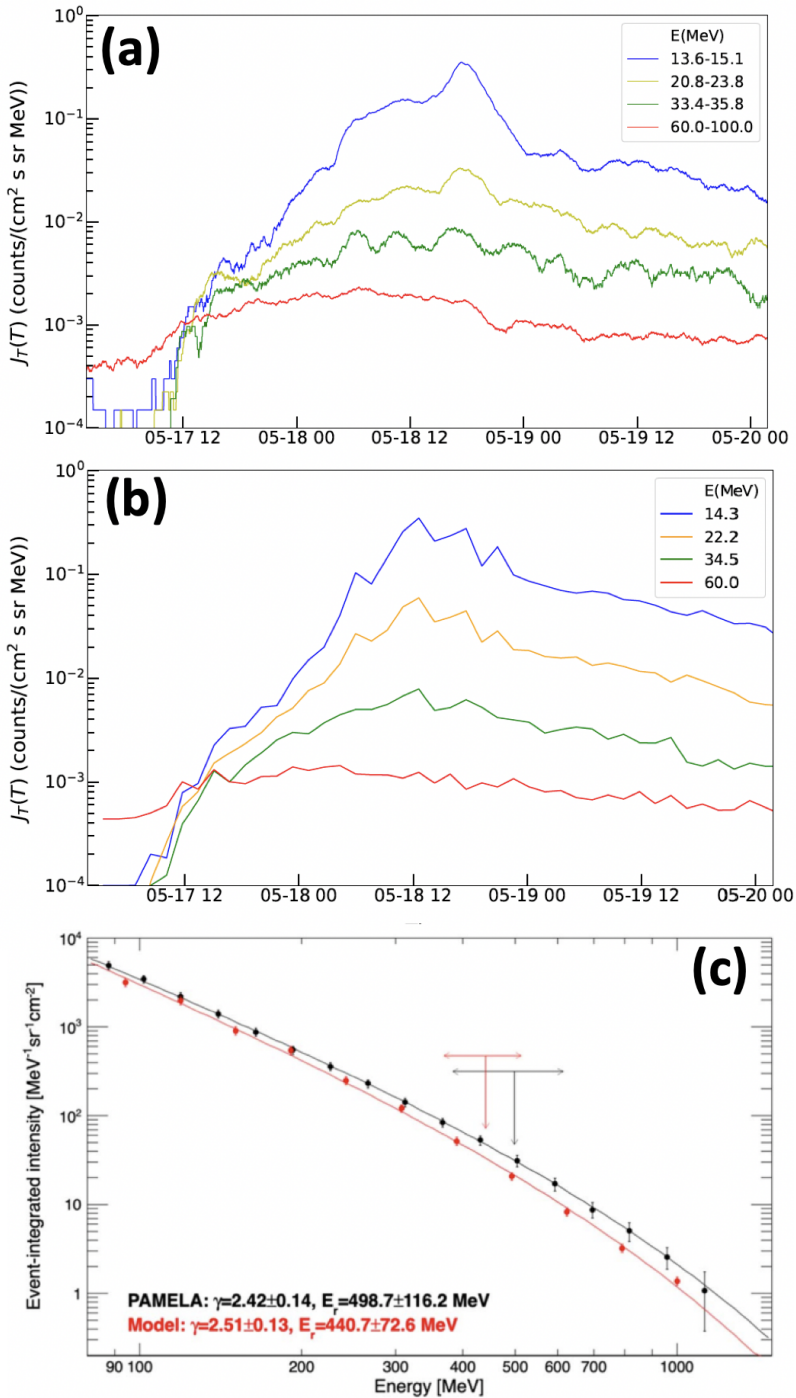


Figure 5. (a) Proton time-intensity profiles for 4 energy bins observed at STEREO-A during the 2012 May 17 SEP event. (b) Modeled proton time-intensity profiles from AWSoM+iPATH. (c) Spectrum comparison between PAMELA observation and model simulation. The black and red arrows indicated the location of the roll-over energies. Figures adapted from Li et al. (2021).

γ -rays in this event. Future studies should self-consistently calculate the transport of back-propagating protons downstream of the CME-driven shock by combining theory and MHD modeling results (e.g., [Petrosian et al. 2023](#)).

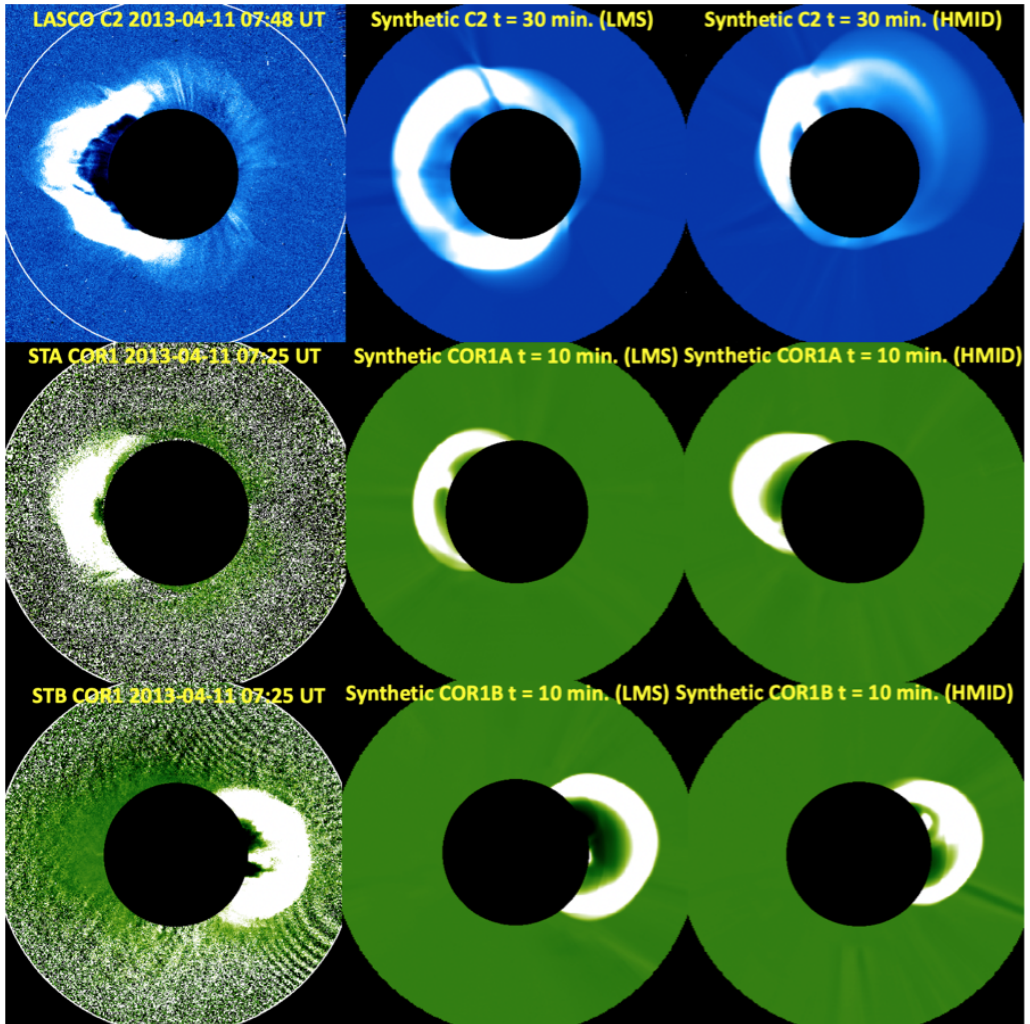


Figure 6. Left: White-light observations from LASCØ C2, STEREO-A COR1 and STEREO-B COR1 of 2013 April 11 CME. Middle: Synthesized white light images from the simulation using Lockheed Martin Synchronic (LMS) map. Right: Synthesized white light images from the simulation using HMI Diachronic (HMID) map.

Finally, we would like to discuss one of the major challenges in CME-driven shock and SEP modeling: the influence of the background solar wind on the properties of the CME-driven shock ([Jin et al. 2022](#)). There are previous studies (e.g., [Hinterreiter et al. 2019](#)) show the uncertainties of the background solar wind modeling. Figure 6 illustrates how the ambient solar corona and wind can significantly affect the parameters of the CME-driven shock. The figure shows the synthesized CME white light images driven by an identical flux rope, but under slightly different background solar wind conditions caused by different types of input magnetic maps (one is a synchronic map, and the other is a diachronic/synoptic map). These variations in the ambient solar wind lead to distinctly different CME-driven shocks. The morphology

of the shock surface shows greater latitudinal expansion in the Lockheed Martin Synchronic (LMS) case than in the HMI Diachronic (HMID) case. The resulting shock parameters are also noticeably different. For detailed comparison of the two cases, we refer to Jin *et al.* (2022). This result underscores the importance of obtaining better constraints on the plasma environment of the CME source region and its path, especially for accurately capturing the early phase of shock evolution.

5. Conclusions

The CME-driven shock plays a crucial role in accelerating particles in the heliosphere. By integrating advanced modeling with multi-messenger observations, we have demonstrated the significant impact CME-driven shocks have on both γ -ray emissions and in-situ SEP observations. Our results provide promising evidence that particles accelerated by CME shocks could travel back to the Sun, producing γ -rays observed by Fermi and potentially opening a new avenue for observing shock-accelerated particles. However, alternative scenarios also exist, and more detailed modeling and observational efforts are required to enhance our understanding of the physical mechanisms behind Fermi SGRE events. By coupling AWSoM with iPATH and involving the early-stage (<10 Rs) shock evolution, our new model shows promising potential to reproduce SEP intensity profiles and spectra at various locations in the heliosphere. Lastly, our findings underscore the importance of accurate background coronal and solar wind modeling, as well as detailed observations of CME source regions, in advancing our understanding of CME-driven shocks and the dynamics of associated energetic particles.

Acknowledgements. M.J., N.N., W.L. acknowledge support from NASA's SDO/AIA contract (NNG04EA00C) to LMSAL. AIA is an instrument onboard the Solar Dynamics Observatory, a mission for NASA's Living With a Star program. The authors also acknowledge support from multiple NASA grants 80NSSC24K0136, 80NSSC21K1782, 80NSSC21K1327, 80NSSC18K1126, and 80NSSC24K0175.

References

- Ackermann, M. *et al.* 2017, Fermi-LAT Observations of High-energy Behind-the-limb Solar Flares. *ApJ*, 835(2), 219.
- Ajello, M. *et al.* 2021, First Fermi-LAT Solar Flare Catalog. *ApJS*, 252(2), 13.
- Atwood, W. B. *et al.* 2009, The Large Area Telescope on the Fermi Gamma-Ray Space Telescope Mission. *ApJ*, 697(2), 1071–1102.
- Axford, W. I., Leer, E., & Skadron, G. The Acceleration of Cosmic Rays by Shock Waves. In *International Cosmic Ray Conference 1977*, volume 11 of *International Cosmic Ray Conference*, 132.
- Borovikov, D., Sokolov, I. V., Manchester, W. B., Jin, M., & Gombosi, T. I. 2017, Eruptive event generator based on the Gibson-Low magnetic configuration. *Journal of Geophysical Research (Space Physics)*, 122(8), 7979–7984.
- Borovikov, D., Sokolov, I. V., Roussev, I. I., Taktakishvili, A., & Gombosi, T. I. 2018, Toward a Quantitative Model for Simulation and Forecast of Solar Energetic Particle Production during Gradual Events. I. Magnetohydrodynamic Background Coupled to the SEP Model. *ApJ*, 864(1), 88.
- Bruno, A., de Nolfo, G. A., Ryan, J. M., Richardson, I. G., & Dalla, S. 2023, Statistical Relationship between Long-duration High-energy Gamma-Ray Emission and Solar Energetic Particles. *ApJ*, 953(2), 187.
- Bruno, A. *et al.* 2018, Solar Energetic Particle Events Observed by the PAMELA Mission. *ApJ*, 862(2), 97.
- Cane, H. V., Mewaldt, R. A., Cohen, C. M. S., & von Roseninge, T. T. 2006, Role of flares and shocks in determining solar energetic particle abundances. *Journal of Geophysical Research (Space Physics)*, 111(A6), A06S90.
- Cane, H. V., von Roseninge, T. T., Cohen, C. M. S., & Mewaldt, R. A. 2003, Two components in major solar particle events. *Geophys. Res. Lett.*, 30(12), 8017.
- Cohen, C., mason, G., Jin, M., Nitta, N., Christian, E., Cummings, A., Desai, M., De Nolfo, G., Giacalone, J., Hill, M., Joyce, C., Labrador, A., Leske, R., Matthaeus, W., McComas, D., McNutt, R., Mewaldt, R., Mitchell, D., Mitchell, J., Rankin, J., Roelof, E., Schwadron, N., Stone, E., Szalay, J., Wiedenbeck, M., Ho, G., & Allen, R. Heavy Ion Characteristics Observed by Multiple Spacecraft Observations in the 28 October 2021 Solar Energetic Particle Event. In *Third Triennial Earth-Sun Summit (TESS) 2022*, volume 54, 2022n7i201p06.
- de Nolfo, G. A., Bruno, A., Ryan, J. M., Dalla, S., Giacalone, J., Richardson, I. G., Christian, E. R., Stochaj, S. J., Bazilevskaya, G. A., Boezio, M., Martucci, M., Mikhailov, V. V., & Munini, R. 2019, Comparing

- Long-duration Gamma-Ray Flares and High-energy Solar Energetic Particles. *ApJ*, 879(2), 90.
- Effenberger, F. & Petrosian, V. 2018, The Relation between Escape and Scattering Times of Energetic Particles in a Turbulent Magnetized Plasma: Application to Solar Flares. *ApJ*, 868(2), L28.
- Gibson, S. E. & Low, B. C. 1998, A Time-Dependent Three-Dimensional Magnetohydrodynamic Model of the Coronal Mass Ejection. *ApJ*, 493, 460–473.
- Gopalswamy, N., Mäkelä, P., Yashiro, S., Lara, A., Xie, H., Akiyama, S., & MacDowall, R. J. 2018, Interplanetary Type II Radio Bursts from Wind/WAVES and Sustained Gamma-Ray Emission from Fermi/LAT: Evidence for Shock Source. *ApJ*, 868(2), L19.
- Gopalswamy, N., Xie, H., Akiyama, S., Yashiro, S., Usoskin, I. G., & Davila, J. M. 2013, The First Ground Level Enhancement Event of Solar Cycle 24: Direct Observation of Shock Formation and Particle Release Heights. *ApJ*, 765(2), L30.
- Gopalswamy, N., Yashiro, S., Mäkelä, P., Xie, H., & Akiyama, S. 2021, The Common Origin of High-energy Protons in Solar Energetic Particle Events and Sustained Gamma-Ray Emission from the Sun. *ApJ*, 915(2), 82.
- Grechnev, V. V., Kiselev, V. I., Kashapova, L. K., Kochanov, A. A., Zimovets, I. V., Uralov, A. M., Nizamov, B. A., Grigorieva, I. Y., Golovin, D. V., Litvak, M. L., Mitrofanov, I. G., & Sanin, A. B. 2018, Radio, Hard X-Ray, and Gamma-Ray Emissions Associated with a Far-Side Solar Event. *Sol. Phys.*, 293(10), 133.
- Hinterreiter, J., Magdalenic, J., Temmer, M., Verbeke, C., Jebaraj, I. C., Samara, E., Asvestari, E., Poedts, S., Pomoell, J., Kilpua, E., Rodriguez, L., Scolini, C., & Isavnin, A. 2019, Assessing the Performance of EUHFORIA Modeling the Background Solar Wind. *Sol. Phys.*, 294(12), 170.
- Hu, J., Li, G., Ao, X., Zank, G. P., & Verkhoglyadova, O. 2017, Modeling Particle Acceleration and Transport at a 2-D CME-Driven Shock. *Journal of Geophysical Research (Space Physics)*, 122(11), 10,938–10,963.
- Hudson, H. S. The Relationship between Long-Duration Gamma-Ray Flares and Solar Cosmic Rays. In Foullon, C. & Malandraki, O. E., editors, *Space Weather of the Heliosphere: Processes and Forecasts 2018*, volume 335, pp. 49–53.
- Jin, M., Manchester, W. B., van der Holst, B., Oran, R., Sokolov, I., Toth, G., Liu, Y., Sun, X. D., & Gombosi, T. I. 2013, Numerical Simulations of Coronal Mass Ejection on 2011 March 7: One-temperature and Two-temperature Model Comparison. *ApJ*, 773, 50.
- Jin, M., Manchester, W. B., van der Holst, B., Sokolov, I., Tóth, G., Mullinix, R. E., Taktakishvili, A., Chulaki, A., & Gombosi, T. I. 2017, a Data-constrained Coronal Mass Ejections in a Global Magnetohydrodynamics Model. *ApJ*, 834a, 173.
- Jin, M., Manchester, W. B., van der Holst, B., Sokolov, I., Tóth, G., Vourlidas, A., de Koning, C. A., & Gombosi, T. I. 2017, b Chromosphere to 1 AU Simulation of the 2011 March 7th Event: A Comprehensive Study of Coronal Mass Ejection Propagation. *ApJ*, 834b, 172.
- Jin, M., Nitta, N. V., & Cohen, C. M. S. 2022, Assessing the Influence of Input Magnetic Maps on Global Modeling of the Solar Wind and CME-Driven Shock in the 2013 April 11 Event. *Space Weather*, 20(3), e2021SW002894.
- Jin, M., Petrosian, V., Liu, W., Nitta, N. V., Omodei, N., Rubio da Costa, F., Effenberg, F., Li, G., Pesce-Rollins, M., Allafort, A., & Manchester, Ward, I. 2018, Probing the Puzzle of Behind-the-limb γ -Ray Flares: Data-driven Simulations of Magnetic Connectivity and CME-driven Shock Evolution. *ApJ*, 867(2), 122.
- Jin, M., Schrijver, C. J., Cheung, M. C. M., DeRosa, M. L., Nitta, N. V., & Title, A. M. 2016, A Numerical Study of Long-range Magnetic Impacts during Coronal Mass Ejections. *ApJ*, 820(1), 16.
- Kozarev, K. A., Evans, R. M., Schwadron, N. A., Dayeh, M. A., Opher, M., Korreck, K. E., & van der Holst, B. 2013, Global Numerical Modeling of Energetic Proton Acceleration in a Coronal Mass Ejection Traveling through the Solar Corona. *ApJ*, 778(1), 43.
- Kozarev, K. A., Korreck, K. E., Lobzin, V. V., Weber, M. A., & Schwadron, N. A. 2011, Off-limb Solar Coronal Wavefronts from SDO/AIA Extreme-ultraviolet Observations—Implications for Particle Production. *ApJ*, 733(2), L25.
- Li, G., Jin, M., Ding, Z., Bruno, A., de Nolfo, G. A., Randol, B. M., Mays, L., Ryan, J., & Lario, D. 2021, Modeling the 2012 May 17 Solar Energetic Particle Event Using the AWSOM and iPATH Models. *ApJ*, 919(2), 146.
- Linker, J. A., Caplan, R. M., Schwadron, N., Gorby, M., Downs, C., Torok, T., Lionello, R., & Wijaya, J. Coupled MHD-Focused Transport Simulations for Modeling Solar Particle Events. In *Journal of Physics Conference Series* 2019, volume 1225 of *Journal of Physics Conference Series*, 012007. IOP.
- Malyshkin, L. & Kulsrud, R. 2001, Transport Phenomena in Stochastic Magnetic Mirrors. *ApJ*, 549(1), 402–415.
- Nitta, N., Jin, M., & Cohen, C. Understanding the Origin of Iron-rich Gradual Solar Energetic Particle Events. In *44th COSPAR Scientific Assembly. Held 16-24 July 2022*, volume 44, 1168.
- Patsourakos, S., Georgoulis, M. K., Vourlidas, A., Nindos, A., Sarris, T., Anagnostopoulos, G., Anastasiadis, A., Chintzoglou, G., Daglis, I. A., Gontikakis, C., Hatzigeorgiu, N., Iliopoulos, A. C., Katsavrias, C., Kouloumvakos, A., Moraitis, K., Nieves-Chinchilla, T., Pavlos, G., Sarafopoulos, D., Syntelis, P., Tsironis,

- C., Tziotziou, K., Vogiatzis, I. I., Balasis, G., Georgiou, M., Karakatsanis, L. P., Malandraki, O. E., Papadimitriou, C., Odstrčil, D., Pavlos, E. G., Podlachikova, O., Sandberg, I., Turner, D. L., Xenakis, M. N., Sarris, E., Tsinganos, K., & Vlahos, L. 2016, The Major Geoeffective Solar Eruptions of 2012 March 7: Comprehensive Sun-to-Earth Analysis. *ApJ*, 817(1), 14.
- Pesce-Rollins, M., Omodei, N., Krucker, S., Di Lalla, N., Wang, W., Battaglia, A. F., Warmuth, A., Veronig, A. M., & Baldini, L. 2022, The Coupling of an EUV Coronal Wave and Ion Acceleration in a Fermi-LAT Behind-the-Limb Solar Flare. *ApJ*, 929(2), 172.
- Pesce-Rollins, M., Omodei, N., Petrosian, V., Liu, W., Rubio da Costa, F., Allafort, A., & Chen, Q. 2015, First Detection of > 100 MeV Gamma Rays Associated with a Behind-the-limb Solar Flare. *ApJ*, 805(2), L15.
- Petrosian, V., Orlando, E., & Strong, A. 2023, Transport of Cosmic-Ray Electrons from 1 au to the Sun. *ApJ*, 943(1), 21.
- Plotnikov, I., Rouillard, A. P., & Share, G. H. 2017, The magnetic connectivity of coronal shocks from behind-the-limb flares to the visible solar surface during γ -ray events. *A&A*, 608, A43.
- Ryan, J. M. & Lee, M. A. 1991, On the Transport and Acceleration of Solar Flare Particles in a Coronal Loop. *ApJ*, 368, 316.
- Sachdeva, N., van der Holst, B., Manchester, W. B., Tóth, G., Chen, Y., Lloveras, D. G., Vásquez, A. M., Lamy, P., Wojak, J., Jackson, B. V., Yu, H.-S., & Henney, C. J. 2019, Validation of the Alfvén Wave Solar Atmosphere Model (AWSoM) with Observations from the Low Corona to 1 au. *ApJ*, 887(1), 83.
- Sokolov, I. V., van der Holst, B., Oran, R., Downs, C., Roussev, I. I., Jin, M., Manchester, Ward B., I., Evans, R. M., & Gombosi, T. I. 2013, Magnetohydrodynamic Waves and Coronal Heating: Unifying Empirical and MHD Turbulence Models. *ApJ*, 764(1), 23.
- Tóth, G., van der Holst, B., Sokolov, I. V., De Zeeuw, D. L., Gombosi, T. I., Fang, F., Manchester, W. B., Meng, X., Najib, D., Powell, K. G., Stout, Q. F., Glocer, A., Ma, Y.-J., & Opher, M. 2012, Adaptive numerical algorithms in space weather modeling. *Journal of Computational Physics*, 231, 870–903.
- Tylka, A. J., Cohen, C. M. S., Dietrich, W. F., Lee, M. A., MacLennan, C. G., Mewaldt, R. A., Ng, C. K., & Reames, D. V. 2005, Shock Geometry, Seed Populations, and the Origin of Variable Elemental Composition at High Energies in Large Gradual Solar Particle Events. *ApJ*, 625(1), 474–495.
- van der Holst, B., Sokolov, I. V., Meng, X., Jin, M., Manchester, IV, W. B., Tóth, G., & Gombosi, T. I. 2014, Alfvén Wave Solar Model (AWSoM): Coronal Heating. *ApJ*, 782, 81.
- Whitman, K. *et al.* 2023, Review of Solar Energetic Particle Prediction Models. *Advances in Space Research*, 72(12), 5161–5242.
- Wijsen, N., Li, G., Ding, Z., Lario, D., Poedts, S., Filwett, R. J., Allen, R. C., & Dayeh, M. A. 2023, On the seed population of solar energetic particles in the inner heliosphere. *Journal of Geophysical Research: Space Physics*, 128(3), e2022JA031203.